± 1.5 kcal/mol for the perdeuteriated species. The former value yields a $Si^+-C_2H_5$ bond energy of 95 ± 2 kcal/mol, which is very close to $D°(Si^+-CH_3)$ = 97 ± 5 kcal/mol.[1] This is consistent with a silicon ion-ethyl structure for this species. The alternate H-$Si^+-C_2H_4$ structure can be further discounted by evaluating the bond energy, $D°(SiC_2H_4^+-H) \leq 99$ kcal/mol. This is much closer to a C-H bond strength than to the Si^+-H bond strength of 75.4 ± 0.9 kcal/mol, although this conclusion is questionable if reaction 3 is very exothermic rather than being thermoneutral.

Acknowledgment. This work was supported by a grant from the National Science Foundation (Grant No. CHE-8917980) and by the Air Force Wright Aeronautical Laboratories. One of the authors (B.H.B.) is grateful to the Korea Science and Engineering Foundation for the partial financial support. We also thank D. K. Bohme for communication of results prior to publication.

van der Waals Complexes of Chemically Reactive Gases: Ozone-Acetylene

J. Z. Gillies,[†] C. W. Gillies,*[,‡] F. J. Lovas,[§] K. Matsumura,[§,⊥] R. D. Suenram,[§] E. Kraka,[∥] and D. Cremer[∥]

Contribution from the Department of Chemistry, Siena College, Loudonville, New York 12211, Department of Chemistry, Rensselaer Polytechnic Institute, Troy, New York 12180, Molecular Physics Division, National Institute of Standards and Technology, Gaithersburg, Maryland 20899, and Theoretical Chemistry, University of Göteborg, Kemigarden 3, S-41296 Göteborg, Sweden. *Received February 12, 1991*

Abstract: A pulsed-beam Fabry-Perot cavity Fourier-transform microwave spectrometer was used to observe rotational spectra of the normal, d_1- and d_2-isotopic species of the ozone-acetylene van der Waals complex. The work employed a modified, pulsed-solenoid valve which served as a flow reactor to sample the reacting gas mixture of 1% ozone and 1% acetylene in argon. The *c*-type transitions of the three isotopic species were split into tunneling doublets due to an internal rotation of acetylene which exchanges the hydrogen (deuterium) atoms. Spectral constants of the two tunneling states for each isotopic species were obtained independently from fits to an asymmetric top Watson Hamiltonian. Stark effect measurements for $O_3-C_2H_2$ gave μ_a = 0.041 (1) and μ_c = 0.473 (1) D. The microwave data show the complex has C_s symmetry with the molecular axis of acetylene located parallel to the OOO plane of ozone at a center-of-mass separation of R_{cm} = 3.251 (2) Å. Ab initio calculations at the MP4(SDQ)/6-31G(d,p) level have found the terminal oxygens of ozone are tilted symmetrically toward the molecular axis of acetylene. The combined microwave and ab initio results indicate that the interaction potential surface of ozone plus acetylene is quite similar to ozone plus ethylene at van der Waals distances.

I. Introduction

Molecular-beam-electric-resonance and pulsed-nozzle Fourier-transform microwave spectroscopies have been used to characterize a large number of van der Waals complexes. The microwave measurements determine the geometries and provide data which can be related to the internal motions of the complexes.[1-3] Generally, these techniques have been applied to the study of weakly bound complexes composed of monomer subunits which do not chemically react with one another. Recently we reported the formation of a van der Waals complex between ozone and ethylene, $O_3-C_2H_4$.[4] In this case, the two monomers are quite reactive with a gas-phase bimolecular rate constant of 1.02×10^6 cm^3 mol^{-1} s^{-1} at room temperature.[5] The $O_3-C_2H_4$ complex was formed in the supersonic expansion obtained from a pulsed-beam valve which was modified so that it sampled a reacting mixture of ozone and ethylene diluted in argon. It was detected in the Fabry-Perot cavity of a Fourier-transform microwave spectrometer.

Since the $O_3-C_2H_4$ complex is located on the reaction potential surface of ozone plus ethylene, the work provided the geometry of a chemical species at large distances along the reaction coordinate. A combination of microwave results and ab initio calculations finds the van der Waals complex has an envelope conformation with C_s symmetry.[6] Ozone plus ethylene is a classical example of a 1,3-dipolar cycloaddition reaction which is thermally allowed by Woodward-Hoffman symmetry rules.[7-10] In the gas phase and solution, the first step in the reaction is concerted and leads to the cycloaddition product 1,2,3-trioxolane ($\overline{CH_2OOO-CH_2}$).[7,8,11] Microwave studies have shown that 1,2,3-trioxolane has a similar oxygen envelope conformation with C_s symmetry[11] as found for the $O_3-C_2H_4$ weakly bound complex.[4,6] Ab initio calculations indicate that the transition-state geometry corresponds to the oxygen envelope conformation.[12] Furthermore, they suggest

[†] Siena College.
[‡] Rensselaer Polytechnic Institute.
[§] National Institute of Standards and Technology.
[⊥] Permanent Address: Seinan Gakuin University, Nishijin, Sawaraku, Fukuoka 814, Japan.
[∥] University of Göteborg.

(1) Dyke, T. R. *Top. Curr. Chem.* **1984**, *120*, 86.
(2) Legon, A. C.; Millen, D. J. *Chem. Rev.* **1986**, *86*, 635.
(3) Novick, S. E. Bibliography of Rotational Spectra of Weakly Bound Complexes. In *Structure and Dynamics of Weakly Bound Molecular Complexes*: Weber, A., Ed.; Reidel Publishing Co.: Dordrecht, Holland, 1987.
(4) Gillies, J. Z.; Gillies, C. W.; Suenram, R. D.; Lovas, F. J.; Stahl, W. *J. Am. Chem. Soc.* **1989**, *111*, 3073.
(5) Herron, J. T.; Huie, R. E. *J. Phys. Chem.* **1974**, *78*, 2085 and references therein.
(6) Gillies, C. W.; Gillies, J. Z.; Suenram, R. D.; Lovas, F. J.; Kraka, E.; Cremer, D. *J. Am. Chem. Soc.* **1991**, *113*, 2412.
(7) Bailey, P. S. *Ozonation in Organic Chemistry*; Academic Press: New York, 1978; Vol. 1; 1982, Vol. 2
(8) Kuczkowski, R. L. *1,3-Dipolar Cycloadditions*; Padwa, A., Ed.; Wiley: New York, 1984.
(9) (a) Woodward, R. B.; Hoffman, R. *The Conservation of Orbital Symmetry*; Verlag Chemie GMSH: Weinheim, 1971. (b) Eckell, A.; Huisgen, R.; Sustmann, R.; Wallbillich, G.; Grashey, D.; Spindler, E. *Chem. Ber.* **1967**, *100*, 2192.
(10) (a) Sustmann, R. *Tetrahedron Lett.* **1971**, *29*, 2717. (b) Sustmann, R. *Pure Appl. Chem.* **1974**, *40*, 569. (c) Houk, K. N.; Sims, J.; Duke, R. E., Jr.; Strozier, R. W.; George, K. *J. Am. Chem. Soc.* **1973**, *95*, 7287. (d) Houk, K. N.; Sims, J.; Watts, C. R.; Luskus, L. J. *J. Am. Chem. Soc.* **1973**, *95*, 7301.
(11) (a) Zozom, J.; Gillies, C. W.; Suenram, R. D.; Lovas, F. J. *Chem. Phys. Lett.* **1987**, *140*, 64. (b) Gillies, J. Z.; Gillies, C. W.; Suenram, R. D.; Lovas, F. J. *J. Am. Chem. Soc.* **1988**, *110*, 7991.

0002-7863/91/1513-6408$02.50/0

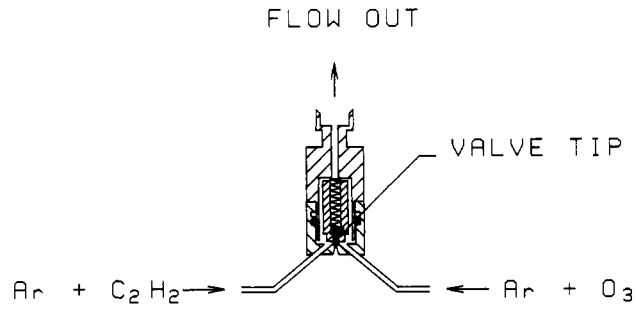

Figure 1. Schematic diagram of the modified, commercial, pulsed-solenoid valve for dual flow of reactive gases.

that the van der Waals complex is located along the reaction coordinate at the entrance to the reaction channel determined by orbital symmetry rules. Hence, it is possible that the orientation of ozone and ethylene in the weakly bound complex influences the formation of the primary product, $\overline{CH_2OOOCH_2}$.

Relatively little is known about the mechanisms of the reaction of ozone with alkynes compared to the ozonolyses of alkenes. For ozone plus acetylene in the gas phase and for solution studies of ozone plus propargyl compounds, the reactions are bimolecular and proceed at rates considerably slower than alkene ozonolyses.[13,14] In the case of ozone plus acetylene, the small rate constant relative to the ozone ethylene reaction is due to a larger activation energy of 10.8 kcal/mol[13] which compares with the ozone plus ethylene activation energy of 5.1 kcal/mol.[5] Unlike the ozonolysis of ethylene, there is no definitive evidence for the corresponding 1,3-dipolar cycloaddition intermediate, 1,2,3-trioxolene (**1**), in the

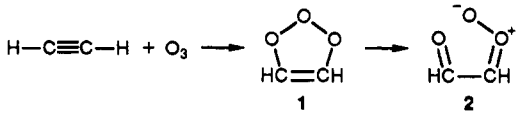

1 **2**

reaction of acetylene with ozone. DeMore finds that a comparison of observed versus calculated preexponential factors for **1** and **2** suggests the formation of **2** to be the rate-determining step. Both **1** and **2**, as well as other species, have been postulated as intermediates in the ozonolyses of alkynes.[13-20] Spectroscopic work[17] and trapping experiments[15,16,18,19,20] provide substantial evidence for the intermediacy of an α-carbonyl carbonyl oxide **2**.

In this paper we report the formation of an ozone–acetylene, O_3–C_2H_2, van der Waals complex employing the modified pulsed-nozzle Fourier-transform microwave spectrometer described in the ozone–ethylene work.[4,6] Microwave spectral data and ab initio calculations are used to show that the structure, internal motion, and stability of the O_3–C_2H_2 complex are very similar to those of the O_3–C_2H_4 complex. The data suggest that the reaction potential surface of ozone plus acetylene does not differ greatly from ozone plus ethylene at van der Waals separations. These results are related to the mechanism of the ozonolysis of acetylene.

II. Experimental Section

The microwave spectra of O_3–C_2H_2, O_3–C_2HD, and O_3–C_2D_2 were recorded using a Balle–Flygare-type[21] Fabry–Perot cavity, Fourier-transform microwave spectrometer described previously.[22] Since acetylene reacts with ozone in the gas phase at room temperature, mixtures of ~1% ozone in argon and 1% acetylene in argon were independently passed through $^1/_{16}$-in. capillary tubing to a modified commercial pulsed solenoid valve (General Valve Corp., Series 9). As shown in Figure 1, the pulsed valve was modified to bring the reactants together on the high-pressure side very near the 0.5-mm orifice. The gases were flowed continuously through the pulsed valve at 1 atm pressure, exiting through the normal gas input which was vented into an exhaust hood. With this design the pulsed valve serves as a flow reactor and as a device to deliver supersonic pulses of the reacting gas mixture to the Fabry–Perot cavity for spectral analysis.

Digital flow controllers were used to regulate the gas flows through the pulsed valve. The argon–acetylene mixture was passed directly from a pressurized gas cylinder through one controller into the pulsed valve. It was preferable not to pass ozone through the controller. Therefore, one of the controllers located between a cylinder of compressed argon and a silica gel trap containing ozone at dry ice temperature regulated the argon–ozone flow into the pulsed valve. Standard procedures employing a Welsbach ozonator were used to prepare ozone from molecular oxygen on the silica gel trap.

Spectral searches for the O_3–C_2H_2 complex were carried out under flow conditions where both acetylene dimer[23] and argon–ozone[24] transitions could be observed readily as single molecular pulse lines. The dual flow method permitted either gas flow to be shut off in order to determine whether transitions required ozone and/or acetylene. Lines assigned to the O_3–C_2H_2 complex were optimized at flow rates of 5 cm^3/min for O_3/Ar and 15 cm^3/min for C_2H_2/Ar. Gas pulses of 200–400-μs duration were delivered into the Fabry–Perot cavity by the modified pulsed valve at repetition rates of up to 35 Hz. Short microwave pulses were used to polarize the O_3–C_2H_2 complex in the cavity when the microwave frequency was close to resonance ($\Delta\nu \leq 0.5$ MHz) with a transition. Free induction decay from the cavity was digitized (512 points, 0.5-μs/point for frequency measurements), and as many as 2000 pulses were averaged to obtain good signal-to-noise ratios for the weaker lines. The averaged data were Fourier-transformed to obtain the power spectrum in the frequency domain with a resolution of 3.9063 kHz/point. Transitions of O_3–C_2H_2 have line widths at half-peak intensities of 12 kHz, and the frequency measurement uncertainty is typically 4 kHz.

The rotational spectrum of O_3–C_2D_2 was observed by using 99% deuterium-enriched acetylene [Cambridge Isotope]. The O_3–C_2HD complex was produced using a sample of acetylene containing approximately 50% C_2HD, 25% C_2H_2, and 25% C_2D_2 (Merck).

Table I. Rotational Transitions of O_3–C_2H_2

transition $J'_{K_{-1},K_{+1}}$–$J''_{K_{-1},K_{+1}}$	state A_1; nuclear spin wt 1		state A_2; nuclear spin wt 3	
	ν_{obsd}[a] (MHz)	$\Delta\nu$[b] (kHz)	ν_{obsd}[a] (MHz)	$\Delta\nu$[b] (kHz)
2_{02}–1_{01}	9832.463	6	9832.441	−1
2_{11}–1_{10}	10434.443	−8	10434.474	3
4_{04} – 3_{12}	10961.494	1	10963.711	2
1_{10}–0_{00}	11780.232	−1	11777.774	3
3_{13}–2_{12}			13930.994	−4
5_{05}–4_{13}	14151.507	0	14153.471	1
3_{03}–2_{02}	14657.390	−5	14657.339	−1
3_{12}–2_{11}			15626.909	1
5_{24}–5_{14}	15604.490	1	15598.363	−2
6_{06}–5_{14}			16708.086	0
4_{23}–4_{13}	16926.309	−4	16920.204	3
2_{11}–1_{01}	17279.990	2	17277.550	2
3_{22}–3_{12}	18010.909	2	18004.832	5
2_{21}–2_{11}	18838.040	−2	18831.986	−11
2_{20}–2_{12}	20572.417	1	20566.461	6
3_{21}–3_{13}	21586.123	1	21580.242	−2
3_{12}–2_{02}	23074.414	−1	23072.011	−3

[a] The frequency measurements have an estimated uncertainty of 4 kHz. [b] $\Delta\nu$ is the observed minus calculated frequency in kHz from the least-squares fit.

III. Results

Microwave Assignments. The geometry of the O_3–C_2H_4 complex[4] was used as a structural model for the O_3–C_2H_2 complex. A near-prolate *c*-type spectrum is predicted with the possibility

(12) (a) McKee, M. L.; Rohlfing, C. M. *J. Am. Chem. Soc.* **1989**, *111*, 2497. (b) Cremer, D.; McKee, M. L. To be published. (c) Dewar, M. J. S.; Hwang, J. C.; Kuhn, D. R. *J. Am. Chem. Soc.* **1991**, *113*, 735.
(13) DeMore, W. B. *Int. J. Chem. Kinet.* **1969**, *1*, 209.
(14) Miller, D. J.; Nemo, T. E.; Hull, L. A. *J. Org. Chem.* **1975**, *40*, 2675.
(15) Criegee, R.; Lederer, M. *Justus Liebigs Ann. Chem.* **1953**, *583*, 29.
(16) Bailey, P. S.; Chang, Y.-G.; Kwie, W. W. L. *J. Org. Chem.* **1962**, *27*, 1198.
(17) DeMore, W. B.; Liu, C.-L. *J. Org. Chem.* **1973**, *38*, 985.
(18) Keary, R. E.; Hamilton, G. A. *J. Am. Chem. Soc.* **1975**, *97*, 6876. Keary, R. E.; Hamilton, G. A. *J. Am. Chem. Soc.* **1976**, *98*, 6578.
(19) Jackson, S.; Hull, L. A. *J. Org. Chem.* **1976**, *41*, 3340.
(20) Jenkins, J. A.; Mendenhall, G. D. *J. Org. Chem.* **1981**, *46*, 3997.
(21) Balle, T. J.; Flygare, W. H. *Rev. Sci. Instrum.* **1981**, *52*, 33.
(22) Lovas, F. J.; Suenram, R. D. *J. Chem. Phys.* **1987**, *87*, 2010. Suenram, R. D.; Lovas, F. J.; Fraser, G. T.; Gillies, J. Z.; Gillies, C. W.; Onda, M. *J. Mol. Spectrosc.* **1989**, *137*, 127.
(23) Fraser, G. T.; Suenram, R. D.; Lovas, F. J.; Pine, A. S.; Hougen, J. T.; Lafferty, W. J.; Muenter, J. S. *J. Chem. Phys.* **1988**, *89*, 6028.
(24) DeLeon, R. L.; Mack, K. M.; Muenter, J. S. *J. Chem. Phys.* **1979**, *71*, 4487.

Table II. Spectral Constants of Ozone–Acetylene Isotopic Species[a]

spectral constants	O_3–C_2H_2		O_3–C_2HD		O_3–C_2D_2	
	A_1 state	A_2 state	B″ state	B′ state	A_1 state	A_2 state
	Rotational and Centrifugal Distortion Constants (MHz)					
A	9030.074 (3)	9027.483 (4)	8623.590 (5)	8624.758 (6)	8220.273 (6)	8219.705 (6)
B	2750.588 (8)	2750.606 (5)	2691.549 (5)	2691.561 (3)	2638.006 (8)	2637.973 (8)
C	2184.177 (9)	2184.160 (6)	2122.917 (4)	2122.940 (3)	2064.648 (12)	2064.695 (12)
Δ_J	0.01764 (6)	0.01766 (5)	0.01668 (11)	0.01733 (13)	0.01587 (9)	0.0158 (1)
Δ_{JK}	0.1101 (4)	0.1104 (2)	0.1012 (2)	0.1016 (1)	0.0965 (5)	0.0981 (5)
Δ_K	−0.059 (1)	−0.177 (1)	−0.142 (1)	−0.082 (2)	−0.082 (2)	−0.127 (2)
δ_J	0.00382 (3)	0.00384 (2)	0.00378 (3)	0.00378[b]	0.00356 (5)	0.00367 (4)
δ_K	0.091 (4)	0.094 (3)	0.089 (2)	0.089[b]	0.090 (5)	0.068 (4)
	Deuterium Hyperfine Constants (kHz)					
eQq_{aa}			−123 (21)	−113 (30)	−99 (4)[c]	
eQq_{bb}			198 (13)	197 (16)	192 (4)[c]	
eQq_{cc}			−74 (15)	−83 (24)	−93.9 (4)[c]	
	Dipole Moment (D)					
$\mu_{(total)}$	0.475 (1)					
μ_a	0.041 (1)					
μ_c	0.473 (1)					

[a] The uncertainties in parentheses are one standard deviation of the least-squares fits. [b] Fixed at this value in the fit. [c] The A_1 and A_2 states of O_3–C_2D_2 are characterized by the same quadrupole coupling constant.

of much less intense *a*-type transitions. Two sets of R-branch and Q-branch *c*-type lines were observed which required both the ozone and acetylene gas flows. Stark effect measurements were employed to make the initial assignments of the rotational quantum numbers. Frequency measurements of these transitions provided spectral constants which were used to locate less intense *a*-type lines. The transition frequencies measured for the two states were least-squares fit to the asymmetrical top Watson Hamiltonian in *I*′ representation and A-reduced form.[25] Table I lists the measured transition frequencies and residuals from the fits for the two states designated A_1 and A_2, respectively. The overall standard deviations of the fits are 2.7 and 5.2 kHz for the A_1 and A_2 states, respectively, which compare well with the estimated frequency measurement uncertainty of 4 kHz. Table II gives the spectral constants obtained from these two fits. The relative intensities of the A_1 and A_2 transitions were approximately 1:3, respectively.

Spectral assignments for both O_3–C_2HD and O_3–C_2D_2 were obtained in the same manner as described above for the normal isotopic species. Each *c*-type transition was split into two states, and the lines were further split as a result of the deuterium electric quadrupole moment. The quadrupole splitting was sufficiently resolved in the two states observed for O_3–C_2HD to measure a number of hyperfine components. The hyperfine splitting due to the single deuterium nucleus of spin $I = 1$ for O_3–C_2HD is the same for the two states designated B″ and B′ in Table III. Quadrupole coupling constants and rotational unsplit line centers were obtained by iteratively fitting the measured hyperfine components listed in Table III using the standard first-order treatment of the nuclear electric quadrupole interaction.[26] The overall standard deviations of the hyperfine structure fits for the B″ and B′ states are 5.9 and 7.2 kHz, respectively. Table II also lists the deuterium quadrupole coupling constants obtained from the fits. The fitted values of eQq_{aa}, eQq_{bb}, and eQq_{cc} for the B″ and B′ states are the same within the experimental uncertainties. Both the B″ and B′ unsplit line centers from the hyperfine fit listed in Table III were least-squares fit to the Watson asymmetric top Hamiltonian in the *I*′ representation and A-reduced form.[25] The rotational constants and quartic centrifugal distortion constants obtained from these fits are given in Table II. Because of the smaller number of lines observed for the weaker B′ state, δ_J and δ_K were fixed at the values obtained for the B″ state of O_3–C_2HD in the least-squares fit of B′ line centers. The overall standard deviations of the B″ and B′ state fits are 1.7 and 2.5 kHz, respectively.

Table III. Rotational Transitions of O_3–C_2HD

transition $J'_{K_{-1},K_{+1}}$–$J''_{K_{-1},K_{+1}}$	F'–F''	state[a] B″; nuclear spin wt 1 ν_{obsd}[b] (MHz)	$\Delta\nu$[c] (kHz)	state[a] B′; nuclear spin wt 1 ν_{obsd}[b] (MHz)	$\Delta\nu$[c] (kHz)
4_{04}–3_{12}		10788.462[d]	0	10787.478[d]	0
	3–2	10788.424	−5	10787.439	−5
	5–4	10788.455	6	10787.469	4
	4–3	10788.505	4	10787.517	−2
1_{10}–0_{00}		11314.818[d]	0	11315.935	0
	1–1	11314.805	6		
	2–1	11314.821	−1		
2_{11}–1_{01}		16696.567	0	16697.687	0
3_{22}–3_{12}		16968.332[d]	0	16970.905[d]	1
	2–2	16968.282	−5	16970.852	−9
	4–4	16968.321	8	16970.894	7
	3–3	16968.384	−4	16970.955	−5
2_{21}–2_{11}		17797.101	0	17799.663	−2
2_{20}–2_{12}		19540.494	−1	19543.021	2
3_{21}–3_{13}		20568.202	1	20570.670	−1
4_{22}–4_{14}		22121.632	−11		
3_{12}–2_{02}		22374.945	0	22376.026	0

[a] B″ is the ground state and B′ designates the less intense higher energy state. [b] The uncertainty in the frequency measurements is estimated to be 4 kHz. [c] $\Delta\nu$ is the observed minus calculated frequency in kHz from the least-squares fit to the coupling constants and the unsplit frequency. [d] Unsplit frequencies obtained from the hyperfine fit.

Structural results presented in a subsequent section of this paper show that the complex has C_s symmetry which means the hydrogen atoms are equivalent. For the O_3–C_2D_2 isotopic species, the two equivalent deuterium nuclei are coupled together to give $I_1 + I_2 = I_D$, where $I_D = 0$, 1, and 2. Coupling of I_D to the overall O_3–C_2D_2 rotational framework gives $F = J + I_D$. Bose–Einstein statistics are obeyed for the pair of deuterium nuclei with nuclear spin of 1. Hence, the symmetric A_1 state wave function must combine with the symmetric $I_D = 0$, 2 nuclear spin wave functions, and the antisymmetric A_2 state wave function combines with the $I_D = 1$ antisymmetric nuclear spin wave function. Since the deuterium nuclei are equivalent by symmetry, one set of deuterium quadrupole coupling constants determines the hyperfine splitting for the observed A_1 and A_2 states. However, the character of the splitting will differ for a given rotational transition of the two states due to the absence of either the $I_D = 0$, 2 or $I_D = 1$ components.[27]

A first-order treatment of the nuclear electric quadrupole interaction for the two equivalent deuterium nuclei was used to

(25) Watson, J. K. G. *Vibrational Spectra and Structure*; Durig, J. R., Ed.; Elsevier: Amsterdam, 1978.
(26) Gordy, W.; Cook, R. L. *Microwave Molecular Spectra*; Wiley: New York, 1970.
(27) Altman, R. S.; Marshall, M. D.; Klemperer, W. *J. Chem. Phys.* **1983**, *79*, 57. Leung, H. O.; Marshall, M. D.; Suenram, R. D.; Lovas, F. J. *J. Chem. Phys.* **1989**, *90*, 700.

Table IV. Rotational Transitions of O_3–C_2D_2

					state A_1; nuclear spin wt 6		state A_2; nuclear spin wt 3	
$J'_{K_{-1},K_{+1}}$–$J''_{K_{-1},K_{+1}}$	F'	I'	F''	I''	ν_{obsd}[a] (MHz)	$\Delta\nu$[b] (kHz)	ν_{obsd}[a] (MHz)	$\Delta\nu$[b] (kHz)
4_{04}–3_{12}					10634.513	0	10634.971	+1
	4	2	3	2	10634.455	−8		
	6	2	5	2	10634.482	−3		
	5	2	4	2	10634.569	11		
	4	1	3	1			10634.928	1
	5	1	4	1			10634.985	−1
1_{10}–0_{00}					10857.908	−2	10857.399	5
	2	2	2	2	10857.879	4		
	1	0	2	2	10857.879	0		
	3	2	2	2	10857.914	−3		
	1	2	2	2	10857.969	0		
	0	1	1	1			10857.355	3
	2	1	1	1			10857.387	−7
	1	1	1	1			10857.426	4
5_{24}–5_{14}					13500.140	−3	13499.068	3
	5	1	5	1			13499.036	8
	6	1	6	1			13499.075	−8
5_{05}–4_{13}					13502.583	0	13502.971	−1
	5	2	4	2	13502.528	0		
	7	2	6	2	13502.552	6		
	6	2	5	2	13502.628	−3		
	5	0	4	0	13502.679	−4		
	4	1	4	1			13502.916	0
	5	1	4	1			13502.916	−3
	6	1	5	1			13502.993	3
4_{23}–4_{13}					14822.812	5	14821.727	−7
	6	2	6	2	14822.782	3		
	5	2	5	2	14822.852	0		
	4	0	4	0	14822.895	−3		
	4	1	4	1			14821.686	3
	5	1	5	1			14821.741	−3
3_{22}–3_{12}					15913.175	1	15912.102	4
	3	2	3	2	15913.107	−8		
	5	2	5	2	15913.136	−4		
	4	2	4	2	15913.239	11		
	3	0	3	0	15913.275	0		
	3	1	3	1			15912.047	−2
	4	1	4	1			15912.121	2
2_{11}–1_{01}					16132.618	2	16132.110	−4
	3	2	3	2	16132.546	−7		
	2	0	1	0	16132.565	0		
	4	2	3	2	16132.643	7		
	1	1	1	1			16132.047	9
	3	1	2	1			16132.102	0
	2	1	2	1			16132.154	−10
2_{21}–2_{11}					16746.963	−6	16745.885	1
	4	2	4	2	16746.929	8		
	3	2	2	2	16746.929	1		
	0	2	1	2	16746.862	−3		
	2	2	2	2	16746.862	−5		
	2	1	2	1			16745.820	8
	3	1	3	1			16745.902	−4
	2	1	1	1			16745.902	−6
	1	1	1	1			16745.960	2
2_{20}–2_{12}					18507.529	6	18506.458	−3
3_{21}–3_{13}					19555.809	−3	19554.809	2
3_{12}–2_{02}					21707.363	0	21706.852	0

[a] The frequency measurements have an estimated uncertainty of 4 kHz. [b] $\Delta\nu$ is the unsplit transition frequency (from the hyperfine fit) minus calculated frequency from the least-squares fit.

iteratively fit the hyperfine lines listed in Table IV and to obtain unsplit line centers. Quadrupole coupling constants obtained from this fit are given in Table II with a standard deviation of 5.0 kHz. The Watson Hamiltonian for an asymmetric top in the I^r representation and A-reduced form[25] was used to fit the unsplit line centers listed in Table IV. This fit included a few lines with unresolved hyperfine components. Table II gives the rotational constants and quartic centrifugal distortion constants obtained from the fit. Overall standard deviations of 6.5 kHz and 6.3 kHz were obtained for the strong A_1 and weak A_2 states, respectively.

Electric Dipole Moment. The dipole moment components μ_a and μ_c were determined from measurements of frequency shifts at applied static electric fields up to 385 V/cm for O_3–C_2H_2. The Stark effect data included a total of 28 measurements of the A_1 and A_2 states on the $M_J = 0$ 1_{10}–0_{00}, the $|M_J| = 0$, 1 2_{11}–1_{01}, and the $|M_J| = 2$, 3 3_{22}–3_{12} transitions. As described previously,[28,29] $\Delta|M_J| = 0$ Stark transitions were observed by applying dc voltages to two parallel plates which were spaced by 26 cm in the cavity and oriented so that the microwave electric field is parallel to the

(28) Campbell, E. J.; Read, W. G.; Shea, J. A. *Chem. Phys. Lett.* **1983**, *94*, 69.
(29) Coudert, L. H.; Lovas, F. J.; Suenram, R. D.; Hougen, J. T. *J. Chem. Phys.* **1987**, *87*, 6290.

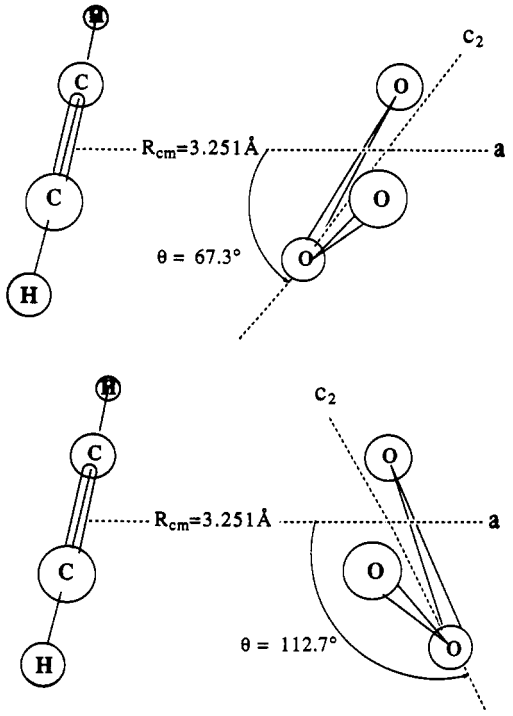

Figure 2. Structures I and II of O_3–C_2H_2 in which the *a,c*-symmetry plane of the complex bisects the C≡C bond of acetylene and the OOO angle of ozone. R_{cm} is the distance from the center of mass of ozone to the center of mass of acetylene, and θ is the angle between R_{cm} and the C_2 axis of ozone. R_{cm} and the C_2 axis of ozone fall in the *a,c* plane.

Table V. Principal Moments of Inertia and Structural Parameters of Free Ozone and Acetylene

monomer	I_a (u·Å²)	I_b (u·Å²)	I_c (u·Å²)
O_3[a]	4.74373	37.8587	42.7038
C_2H_2[b]		14.3273	
	Monomer Geometry		
O_3[c]	R(O–O) = 1.276 Å	θ(OOO) = 116.97°	
C_2H_2[d]	R(C–H) = 1.057 Å	R(C≡C) = 1.208 Å	

[a] Calculated from the rotational constants listed in ref 32. [b] Calculated from the rotational constant listed in ref 33. [c] R(O–O) and θ(OOO) were obtained from an r_0 fit of the moment data of the normal isotopic species of ozone reported in ref 32. [d] R(C–H) and R(C≡C) were determined from an r_0 fit of the moment data of C_2H_2, C_2HD, and C_2D_2 reported in: Fast, H.; Welch, H. L. *J. Mol. Spectrosc.* **1972**, *41*, 203, and in ref 33.

dc electric field. The effective static electric field between the plates was determined using the Stark effect of the J = 1–0 transition of OCS and its known electric dipole moment of 0.715 19 (3) D.[30]

Frequency shifts were quadratic with respect to the static electric field for all the transitions noted above. The Stark effect data, including both the A_1 and A_2 states, were least-squares fit to second-order perturbation theory,[31] giving μ_a = 0.041 (1) and μ_c = 0.473 (1) D with a standard deviation of 3.1 kHz for the overall fit. The absence of *b*-type transitions in conjunction with the quality of this fit indicate that the complex has an *a,c* plane of symmetry. Table II lists the total electric dipole moment and the components along the *a* and *c* inertial axes of O_3–C_2H_2.

Structural Analysis. The observation of *a*- and *c*-dipole transitions and the electric dipole measurements are consistent with an *a,c* plane of symmetry for O_3–C_2H_2. While there are a number of structures which satisfy this symmetry constraint, only the two forms shown in Figure 2 are in agreement with the moment of inertia data. The observed out-of-plane second moment, P_{bb} = $1/2(I_a + I_c - I_b)$ = 51.8 u·Å², for O_3–C_2H_2 is very close to the sum of I_b(ozone) + I_b(acetylene) = 52.2 u·Å² (see Table V),[32,33] which indicates the two carbons and terminal oxygens of ozone are located out of the *a,c* plane. All other forms consistent with the symmetry constraint have calculated values of P_{bb} which are too small because of the location of either the carbon atoms or oxygen atoms in the *a,c* symmetry plane.

Table VI. Comparison of r_0 with Substitution Coordinates of Hydrogen Atoms in the Ozone–Acetylene Complex

	atomic coordinates (Å)		
	a	*b*	*c*
structure I (r_0)[a]	−2.108	±1.661	−0.0204
structure II (r_0)[a]	−2.108	±1.661	+0.0204
O_3–C_2H_2/O_3–C_2HD (r_s)[b]	1.995	1.657	0.0689
O_3–C_2H_2/O_3–C_2D_2 (r_s)[b]	2.003	1.658	0.1084

[a] The hydrogen coordinates were obtained from least-squares fits of the moment of inertia data to the two structural parameters R_{cm} and θ. [b] The monosubstituted and disubstituted deuterium isotopes give the magnitude but not the sign of the hydrogen coordinates by the Kraitchman and Chutjian methods.

If it is assumed that the geometries of ozone and acetylene are not changed upon complexation, there are two coordinates necessary to determine the structure of the complex as shown in Figure 2. These coordinates are defined as R_{cm}, the distance between the center of mass of ozone and acetylene, and θ, the angle between R_{cm} and the C_2 axis of ozone. With the geometries of the monomers fixed at the values listed in Table V, the combined nine moments of inertia of the A_1 states of O_3–C_2H_2 and O_3–C_2D_2 and the B″ state of O_3–C_2HD were least-squares fit to obtain R_{cm} and θ. There are two sets of (R_{cm}, θ) coordinates which satisfy the moment of inertia data. These sets give R_{cm} = 3.251 (2) Å and θ = 67.3 (34)° or θ = 112.7 (34)° which correspond to the structures designated I and II in Figure 2. In both fits the moment of inertia data fit with an overall standard deviation of σ = 0.43 u·Å². Structure I tilts the central oxygen of ozone toward acetylene, whereas structure II locates the terminal oxygens of ozone closest to acetylene. Fits of the six moments of inertia for the isotopic pairs O_3–C_2H_2, O_3–C_2HD and O_3–C_2H_2, O_3–C_2D_2 do not resolve the ambiguity in θ and also yield values of R_{cm} and θ which are within the experimental uncertainties of these parameters obtained in the nine moment fits.

Since ^{18}O substitution in ozone does not appear to be feasible owing to the expense associated with the flow requirements, the microwave data do not resolve the ambiguity in the angle, θ. Structures I and II differ in the sign but not the magnitude of the small *c* hydrogen coordinates of O_3–C_2H_2. Unfortunately, the substitution method does not determine the sign of atomic coordinates calculated from isotopic moment of inertia data and is not reliable for small coordinates less than 0.15 Å.[26] These problems can be seen in Table VI which compares the substitution coordinates of hydrogen obtained from both O_3–C_2HD via Kraitchman's equations[34] and O_3–C_2D_2 via Chutjian's equations[35] to the fitted r_0 atomic coordinates. There is poor agreement between the substitution and fitted values of the *c* hydrogen coordinate because of the small coordinate problem mentioned above. However, the agreement is good between the r_0 hydrogen *a* and *b* coordinates of structures I and II, and those determined via the substitution methods.

The dipole moments along the inertial axes of O_3–C_2H_2 can be calculated for structures I and II using the known electric dipole moment of free ozone (μ_{total} = μ_b = 0.5324 D).[32] Projections of the O_3 dipole moment for θ = 67.3° (structure I) and θ = 112.7° (structure II) give μ_a(complex) = 0.205 D and μ_c(complex) = 0.491 D. Only the direction of μ_a(complex) differs between structures I and II owing to the opposite projections of the ozone

(30) Reinhartz, J. M. L. J.; Dymanus, A. *Chem. Phys. Lett.* **1974**, *24*, 346.
(31) Golden, S.; Wilson, E. B. *J. Chem. Phys.* **1948**, *16*, 669.
(32) Lovas, F. J. *J. Phys. Chem. Ref. Data* **1978**, *7*, 1445.
(33) Palmer, K. F.; Michelson, M. E.; Rao, K. N. *J. Mol. Spectrosc.* **1972**, *44*, 131.
(34) Kraitchman, J. *Am. J. Phys.* **1953**, *21*, 17.
(35) Chutijan, A. *J. Mol. Spectrosc.* **1964**, *14*, 361.

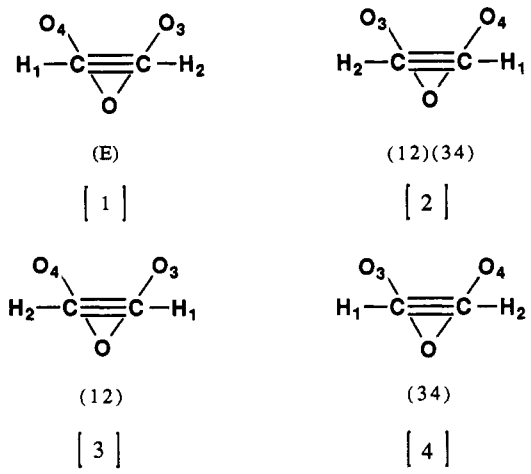

Figure 3. Four equivalent frameworks of O_3–C_2H_2 designated as [1], [2], [3], and [4]. The complex is projected approximately in the *b,c* plane with ozone located behind acetylene. The permutation inversion operation to be applied upon the basis function of framework [1] is given in parentheses under that framework.

dipole moment along the *a* principal axis of O_3–C_2H_2 (see Figure 2). Since the experimental measurements of μ_a(complex) and μ_c(complex) do not determine the signs of the dipole moment components, these data also do not distinguish structure I from structure II.

Internal Motions. The *a*- and *c*-type transitions of O_3–C_2H_2 are split into two states, designated A_1 and A_2, due to an internal motion in the complex. Two tunneling states are also found for the observed *c*-type transitions of O_3-C_2HD and O_3–C_2D_2. The lines are pure rotational transitions and fit a Watson Hamiltonian to within the experimental uncertainty of the frequency measurements. The observed relative intensities for the two states are consistent with nuclear spin statistical weights of 1:3 and 6:3 for the A_1 and A_2 states of O_3–C_2H_2 and O_3–C_2D_2, respectively, which indicate the hydrogens (deuteriums) are exchanged by the tunneling motion. Additional evidence for the hydrogen exchange in the tunneling motion comes from the observed deuterium hyperfine splittings for O_3–C_2HD and O_3–C_2D_2 transitions. Both the B″ and B′ states of O_3–C_2HD have the same hyperfine pattern for a given rotational transition. In contrast, the A_1 state lines of O_3–C_2D_2 contain the I_D = 0, 2 components, while the A_2 state lines consist of only the I_D = 1 components (see Table IV). Finally, the A_1,A_2-state splittings are reduced by deuteration in the complex. This effect can be seen by noting that the difference between the *A* rotational constants of the A_1 and A_2 states is 2.59 MHz for O_3–C_2H_2 and 0.54 MHz for O_3–C_2D_2 (see Table II).

Since the complex has an *a,c* symmetry plane which bisects the C≡C bond of acetylene and the OOO angle of ozone, four equivalent frameworks are possible for O_3–C_2H_2 and O_3–C_2D_2. As shown in Figure 3, tunneling motions between these frameworks exchange the hydrogen nuclei of acetylene and the terminal oxygens of ozone. The [1] → [2] motion interchanges the hydrogens and oxygens by a geared internal rotation of both monomers, the [1] → [3] motion interchanges the hydrogen nuclei through an internal rotation of acetylene, and the [1] → [4] motion interchanges the oxygens by an internal rotation of ozone.

Both O_3–C_2H_2 and O_3–C_2D_2 have the same permutation-inversion group as H_2O–D_2O.[29,36] By analogy to H_2O–D_2O, each asymmetric rotor level is split into four states by the motions in Figure 3. The symmetry species of the four states are $A_1^{\pm}$, $A_2^{\pm}$, $B_1^{\pm}$, and $B_2^{\pm}$. Selection rules for the allowed transitions are $A_1^{\pm} \leftrightarrow A_1^{\pm}$, $A_2^{\pm} \leftrightarrow A_2^{\pm}$, $B_1^{\pm} \leftrightarrow B_1^{\pm}$, and $B_2^{\pm} \leftrightarrow B_2^{\pm}$. Because of the exchange of spin $^1/_2$ protons and spin 0 oxygen nuclei, nuclear spin weights of g = 1, 3, 0, 0 (O_3–C_2H_2) and g = 6, 3, 0, 0 (O_3–C_2D_2) are obtained for the A_1, A_2, B_1, and B_2 states, respectively. The tunneling motions will give only two observable states, A_1 and A_2, since the B_1 and B_2 states have zero spin weights. The same result is obtained for the [1] → [2] motion which produces the two states A_1 and A_2 with spin weights g = 1:3, respectively. Thus, both the [1] → [2] and [1] → [3] motions are consistent with the observation of the two states having spin weights g = 1 (A_1) and g = 3 (A_2) for O_3–C_2H_2 and g = 6 (A_1) and g = 3 (A_2) for O_3–C_2D_2. An exchange of the hydrogen and terminal oxygen nuclei can also be obtained through a concerted internal rotation of acetylene and inversion of ozone along its C_2 axis. This tunneling pathway also connects frameworks [1] and [2] but would invert the μ_c dipole component of the complex in contrast to the geared internal rotation of both monomer subunits. This would cause the K_a = even and K_a = odd levels to be shifted in opposite directions by the tunneling frequency ν_T, and the *c*-type transitions would be offset from the rigid rotor positions by $\pm 2\nu_T$. Since this was not observed, there is no evidence for the geared motion which involves the inversion of ozone.

Because of the lower symmetry of O_3–C_2HD, it cannot be treated with O_3–C_2H_2 and O_3–C_2D_2. However, four isoenergetic frameworks are possible for O_3–C_2HD and by analogy to HDO–DOD which is represented by the same permutation-inversion group each asymmetric rotor level splits into four components. The symmetry species of these components are $A^{\pm}$ and $B^{\pm}$. Selection rules follow $A^{\pm} \leftrightarrow A^{\pm}$ and $B^{\pm} \leftrightarrow B^{\pm}$. The nuclear spin weights of the pairs of A and B states are g = 0 and g = 1, respectively. Since only the two B states have nonzero spin weights, the tunneling motion will split the rotational transitions into two states. This is consistent with the observation of two states, designated B″ and B′ in Table III, for O_3–C_2HD.[37] Relative intensities of rotational transitions of the B″ and B′ states will depend only upon the difference in energy of the two states. Hence, the more intense B″ state is assigned to the ground state.

The transition frequency splittings, observed relative intensities consistent with nuclear spin weights, and deuterium hyperfine effects strongly suggest that the motion involves an internal rotation of acetylene which exchanges the hydrogen nuclei. However, it is not certain whether the oxygen nuclei are also exchanged by an internal rotation of ozone. Therefore, the data do not distinguish the [1] → [2] from the [1] → [3] motion in Figure 3. Unfortunately, oxygen-18 enriched ozone studies of the complex which might resolve this problem of the tunneling path do not appear feasible owing to the flow requirements for the reactive gas mixture.

Theoretical Results. Various levels of theory ranging from Hartree–Fock (HF) to fourth-order Moller–Plesset (MP) perturbation theory[38] have been used together with the 6-31G(d,p) basis set[39] to investigate the O_3–C_2H_2 complex. For a reasonable description of a van der Waals complex, it is necessary to correctly evaluate the electrostatic interaction between the monomer subunits. This implies an accurate determination of the multipole moments, in particular, atomic charges and dipole moments, of the molecules combined in the complex. In a previous investigation we found that a reasonable description of the ozone dipole moment is obtained at the MP4(SDQ) level due to cancellation of errors.[40] The HF value of the dipole moment of ozone is too large, and the MP2 value is too small, thus leading to either an over- or an underestimation of the stability of ozone van der Waals complexes. The MP3 and MP4(SDTQ) dipole moments of ozone are better, but closest agreement with experiment[32] is obtained at the MP4(SDQ) and the QCISD level of theory.[40] QCI calculations for the ozone-acetylene complex are not feasible and, therefore, we have chosen MP4(SDQ) to describe the complex. At the MP4(SDQ)/6-31G(d,p) level of theory, a complete geometry

(36) Coudert, L. H.; Hougen, J. T. *J. Mol. Spectrosc.* **1988**, *130*, 86.

(37) The prime and double prime designations of the B states for O_3–C_2HD have no group theoretical significance but rather serve to distinguish the two sets of rotational transitions.

(38) (a) Moller, C.; Plesset, M. S. *Phys. Rev.* **1934**, *46*, 618. (b) Pople, J. A.; Binkley, J. S.; Seeger, R. *Int. J. Quantum Chem.* **1976**, *10*, 1. (c) Krishnan, R.; Pople, J. A. *Int. J. Quantum Chem.* **1978**, *14*. 91. (d) Krishnan, R.; Frisch, M. J.; Pople, J. A. *J. Chem. Phys.* **1980**, *72*, 4244.

(39) Hariharan, P. C.; Pople, J. A. *Chem. Phys. Lett.* **1972**, *66*, 217.

(40) Cremer, D.; Kraka, E. To be published.

Table VII. Comparison of Calculated and Experimental Geometries and Electric Dipole Moments of the Ozone–Ethylene and Ozone–Acetylene Complexes

	ozone–ethylene[b]		ozone–acetylene	
parameter[a]	MP4(SDQ) 6-31G(d,p)	exptl[c]	MP4(SDQ) 6-31G(d,p)	exptl[c]
R(OO)	1.269	(1.276)	1.268	(1.276)
R(CC)	1.336	(1.339)	1.212	(1.208)
R(C–H)	1.081	(1.086)		
	1.080		1.062	(1.057)
∠OOO	117.4	(117.0)	117.4	(117.0)
∠CCH	121.7	(121.1)		
	121.7			
R_{cm}[d]	3.116	3.290	3.106	3.251
θ_1[d]	109.8	112.0	105.6	112.7
θ_2[e]	98.8	106.0		
μ	0.499	0.466	0.529	0.475
μ(corrected)[f]	0.46		0.49	

[a] Distances R are given in Å, angles θ in deg, dipole moment μ in debyes. [b] Reference 6. [c] Values in parentheses are r_0 parameters derived from the experimental moments of inertia of ozone and acetylene (listed in Table V) and ethylene (see ref 6). [d] R_{cm} and θ_1 are defined in Figure 2 and ref 6. [e] θ_2 is the angle between R_{cm} and the molecular plane of ethylene (see Figure 1 in ref 6). [f] At the MP4(SDQ) level of theory the monomer dipole moment of ozone is calculated to be 0.04 D higher than the experimental value of 0.53 D. Subtracting 0.04 D from the MP4(SDQ) dipole moments of O_3–C_2H_4 and O_3–C_2H_2 gives μ(corrected).

optimization of the two C_s symmetry forms of O_3–C_2H_2 (designated I and II in Figure 2) was carried out using analytical gradients.[41]

In Table VII the MP4(SDQ) geometry of O_3–C_2H_2 is compared with the experimental structure of O_3–C_2H_2 as well as with the corresponding geometries reported previously for O_3–C_2H_4.[6] Although small differences between the equilibrium r_e geometry determined at the MP4(SDQ) level and the experimental r_0 structure are present, a number of conclusions can be made from the data in Table VII. In the MP4(SDQ) O_3–C_2H_4 and O_3–C_2H_2 structures the monomer geometries differ only by a small amount from the free monomer structures. Therefore, it is reasonable to use the experimental r_0 geometries of the monomers when determining the structure of the van der Waals complex, O_3–C_2H_2, from the microwave moment of inertia data. The MP4(SDQ) geometry of the O_3–C_2H_2 complex clearly suggests that the structure observed experimentally is structure II in Figure 2. According to theory, structure I is 1.7 kcal/mol less stable than structure II. Optimization of structure I leads either to II or to dissociation into ozone and acetylene. Finally both theory and experiment indicate that the geometry of the O_3–C_2H_2 complex is very similar to that of the O_3–C_2H_4 complex.

Comparison of calculated and experimentally observed geometries of the O_3–C_2H_2 complex reveals that R_{cm} is predicted 0.15 Å and θ 7° too small by theory. These discrepancies which have also been found for the O_3–C_2H_4 complex[6] arise in part from differences in r_e and r_0 geometries owing to the effect of large amplitude motions. However, the fact that a basis set of moderate size has been used for the van der Waals complex, while for high accuracy at least a TZ + 2P basis is needed, suggests that the discrepancies also are due to basis set limitations. MP4/TZ + 2P calculations for a five heavy atom system are presently not feasible. Nevertheless, the method used allows a reasonable description of stability, geometry, and electronic structure of the complex.

This is also reflected by the calculated MP4(SDQ) dipole moment of 0.53 D for the O_3–C_2H_2 complex. At the MP4(SDQ) level of theory the monomer dipole moment of ozone is 0.04 D larger than the experimental monomer value of 0.53 D.[32] Subtracting 0.04 D from the MP4(SDQ) value of the O_3–C_2H_2 dipole moment gives 0.49 D which is in good agreement with the experimental value of 0.475 D. Even better agreement is obtained by applying the 0.04 D correction to the MP4(SDQ) value of 0.499 D for the O_3–C_2H_4 dipole moment (see Table VII).

The binding energy of the O_3–C_2H_2 complex has been calculated by making the appropriate corrections for basis set superposition errors (BSSE). At the MP4(SDQ) level, the binding energy is 0.85 kcal/mol. This compares closely to the binding energy of 0.74 kcal/mol calculated for the O_3–C_2H_4 complex at the MP4(SDQ) level of theory. The stability and geometry of the O_3–C_2H_2 complex is predominantly determined by electrostatic interactions rather than charge transfer or overlap interactions, which are negligibly small at a distance of 3 Å. In the complex the two molecules adopt positions that allow a maximum electrostatic attraction between the partially positive H atoms of acetylene and the partially negative terminal O atoms of ozone. Since the interaction between electron lone pairs of the central O atom of ozone and the π electrons of acetylene is repulsive, structure II with θ = 112.7° is preferred.

IV. Discussion

Structural and Internal Dynamics. The O_3–C_2H_2 van der Waals complex is quite similar to the O_3–C_2H_4 complex. The conformations are virtually the same with the a,c symmetry planes bisecting the C=C and C≡C bonds of ethylene and acetylene as well as the OOO angle of ozone. With θ_1 = 112 (4)° in O_3–C_2H_4 and θ = 112.7 (34)° in O_3–C_2H_2 (see Figure 2), ozone has the same tilt with respect to the center of mass separation, R_{cm}, in the two complexes. This tilt places the terminal oxygen of ozone rather than the central oxygen closest to the C–H bond in acetylene (~3.21Å) and the C–H_{exo} bond in ethylene (~3.20 Å). Also, R_{cm} = 3.290 (3) Å in O_3–C_2H_4 which differs by only 0.04 Å from R_{cm} = 3.251 (2) Å in O_3–C_2H_2.

Striking similarities are also found in the binding energies and internal dynamics of the two complexes. The BSSE corrected values calculated at the MP4(SDQ)/6-31G(d,p) level of theory are 0.74 kcal/mol and 0.85 kcal/mol for O_3–C_2H_4 and O_3–C_2H_2, respectively. Estimates of the van der Waals bond stretching force constant from the quartic centrifugal distortion constant, Δ_J, give values of 0.0318 mdyn/Å and 0.0354 mdyn/Å, respectively, for O_3–C_2H_4[6] and O_3–C_2H_2. These results are consistent with ab initio calculations of the binding energies since they indicate that the van der Waals interactions are qualitatively about the same for O_3–C_2H_4 and O_3–C_2H_2.

Two tunneling states are observed for O_3–C_2H_4 and O_3–C_2H_2. In both cases the tunneling splitting is small (approximately 10 MHz and 5 MHz, respectively, for the 1_{10}–0_{00} transitions of O_3–C_2H_4 and O_3–C_2H_2), and the two states for each complex fit independently quite well to an asymmetric top Watson Hamiltonian. The spectral evidence is consistent with an internal motion which exchanges the hydrogens by rotation of ethylene or acetylene about a C_2 axis that is perpendicular to the molecular plane of ethylene or the molecular axis of acetylene. In the case of O_3–C_2H_4, ab initio calculations provide a 0.4-kcal/mol estimate of the barrier to the internal rotation of ethylene described above.[6]

Recent studies of the SO_2–C_2H_4 and SO_2–C_2H_2 van der Waals complexes have found somewhat similar structures.[42,43] Like O_3–C_2H_4 and O_3–C_2H_2, a,c symmetry planes bisect the OSO angle and the C=C and C≡C bonds in the two complexes. However, the SO_2 and O_3 tilts are in the opposite sense with respect to R_{cm}. With θ_1 = 80° in SO_2–C_2H_4[42] and θ_1 = 76° in SO_2–C_2H_2,[43] the sulfur atom is tilted toward the C=C and C≡C bonds. This differs from O_3–C_2H_4 and O_3–C_2H_2 where the terminal oxygens of ozone are tilted toward the C=C and C≡C bonds. Also, unlike O_3–C_2H_4, the SO_2 plane is nearly parallel to the ethylene plane for SO_2–C_2H_4.[6,42]

Both the van der Waals bond stretching force constants in SO_2–C_2H_4 (0.057 mdyn/Å)[42] and SO_2–C_2H_2 (0.047 mdyn/Å)[43] are larger than the values obtained for O_3–C_2H_4[6] and O_3–C_2H_2

(41) (a) Gauss, J.; Cremer, D. *Chem. Phys. Lett.* **1988**, *138*, 131. (b) Gauss, J.; Cremer, D. *Chem. Phys. Lett.* **1989**, *153*, 303.

(42) Andrews, A. M.; Taleb-Bendiab, A.; LaBarge, M. S.; Hillig II, K. W.; Kuczkowski, R. L. *J. Chem. Phys.* **1990**, *93*, 7030.

(43) Andrews, A. M.; Hillig, K. W.; Kuczkowski, R. L.; Legon, A. C.; Howard, N. W. *J. Chem. Phys.*, submitted for publication.

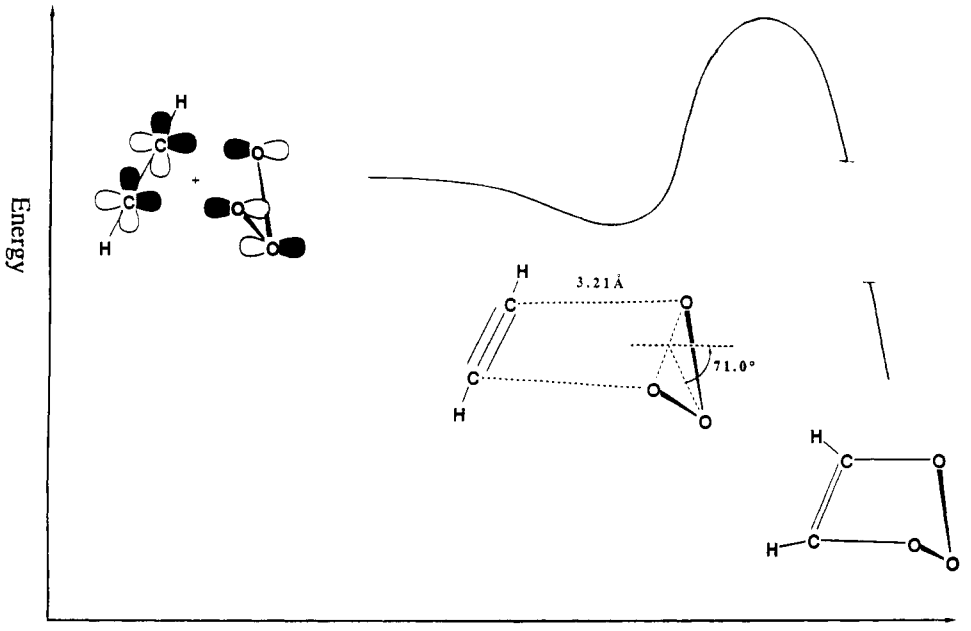

Figure 4. The one-dimensional reaction potential surface of ozone plus acetylene defined by 1,3-dipolar cycloaddition theory.

which suggest stronger van der Waals interactions in the SO_2 complexes. The force constants indicate that SO_2–C_2H_2 is less strongly bound than SO_2–C_2H_4. These results are not consistent with the ab initio calculations of the binding energies of SO_2–C_2H_2 (2.6 kcal/mol) and SO_2–C_2H_4 (2.5 kcal/mol).[43] They also differ from the trend found for the ozone-containing complexes where the force constants and ab initio calculations suggest that O_3–C_2H_2 (0.85 kcal/mol) is more strongly bound than O_3–C_2H_4 (0.74 kcal/mol). The ab initio calculations of the SO_2 ethylene and acetylene complexes employed limited basis sets and were not corrected for BSSE. Therefore, the binding energies of these complexes are too large, exaggerating the true differences in the stabilities of the SO_2 and O_3 ethylene and acetylene complexes.

The internal motion in SO_2–C_2H_4 is quite similar to O_3–C_2H_4 and involves the analogous internal rotation of ethylene about its C_2 axis perpendicular to the molecular plane of ethylene.[42] Tunneling doublets are found with small splittings which are not larger than typically a factor of 2 compared to those observed in O_3–C_2H_4.[6] Surprisingly, tunneling doublets have not been found for SO_2–C_2H_2 which suggests that the barrier to internal rotation of acetylene is considerably higher in SO_2–C_2H_2 than in O_3–C_2H_2. This seems contradictory to the conclusion that SO_2–C_2H_2 is more weakly bound than SO_2–C_2H_4 based on the force constants.

Reaction Potential Surface. Although ozone reacts with acetylene, little is known about the mechanism. The first step may be viewed as a 1,3-dipolar cycloaddition. As shown in Figure 4, a parallel plane approach of ozone and acetylene allows for maximum overlap between the π^* LUMO orbital of ozone and π HOMO orbital of acetylene.[7-10] It leads to the cycloaddition product 1,2,3-trioxolene via a transition state which falls along the reaction coordinate defined in Figure 4. The parallel plane orientation of the reacting molecules is maintained along this reaction coordinate. This means the van der Waals complex observed in the present work must fall in a shallow minimum at large reactant distances on this reaction coordinate because its geometry corresponds to the C_s symmetry of the cycloaddition pathway. Ab initio calculations find the parallel plane transition state to be 10 kcal/mol higher in energy than the reactants.[44]

DeMore's Arrhenius plot of ozone plus acetylene kinetic data gives an activation energy, E_a, of 10.8 kcal/mol[13] which is in reasonable agreement with the ab initio calculations of a 1,2,3-trioxolene transition state. However, the preexponential factor, A, calculated by DeMore for a ring-like transition state ($A = 10^{7.2}$ M^{-1} s^{-1}) is too low when compared to the observed A of $10^{9.5}$ M^{-1} s^{-1}. Much better agreement with the experimental value is obtained for an open chain-like transition state. Consequently, DeMore's data suggest that O–O bond-breaking in going from 1,2,3-trioxolene, (**1**) to α-carbonyl carbonyl oxide, (**2**) is the rate-determining step.

DeMore's kinetic rate data are consistent with a 1,2,3-trioxolane transition state for the rate-determining step of ozone plus ethylene.[13] The second step in the mechanism of ozone plus ethylene is postulated to be a concerted 1,3-dipolar cycloreversion of 1,2,3-trioxolane in which the CC and OO bonds are broken to give formaldehyde plus carbonyl oxide.[7,8] For ozone plus acetylene, this step involves simply breaking the OO bond to give **2**. Work is in progress to investigate the early steps of the ozonolysis of acetylene employing a combination of theoretical and low-temperature millimeter wave spectroscopic techniques.

Acknowledgment. D.C. and E.K. thank the Swedish Natural Science Research Council (NFR) for financial support and the Nationellt Superdatorcentrum (NSC), Linköping, Sweden, for a generous allotment of computer time. All the ab initio calculations have been performed on the CRAY XMP 48 of the NSC. We are grateful to Dr. L. H. Coudert for helpful discussions related to the group theoretical aspects of the tunneling motion and for software used in the O_3–C_2D_2 hyperfine analysis. This research was partially supported by a grant from Research Corporation (C.W.G.).

(44) Cremer, D. To be published.